

From waste to treat waste: exploitation of marble dust as a harmful pollutant to a green adsorbent for dyes and heavy metals from industrial wastewater

H.A. Attia ¹, Mohamed G. Farghaly ¹, A.M. Saleh ², M.A. Abdel Khalek ³

¹ Al-Azhar University, Faculty of Engineering, Mining and Petroleum Engineering Department, Qena, Egypt

² Al-Azhar University, Faculty of Engineering, Mining and Petroleum Engineering Department, Cairo, Egypt

³ Central Metallurgical Research & Development Institute (CMRDI), Helwan, Cairo, Egypt.

Corresponding author: kalekma@yahoo.com

Abstract: The marble dust as a harmful industrial waste of marble fabrication was evaluated as an economical and efficient green adsorbent for Acid Red-1 dye and lead ions. The XRD, XRF, particle size, surface area and zeta-potential measurements were used to characterize the marble dust. The removal efficiency was optimized by studying several parameters such as pH, temperature, contact time, adsorbent dose and initial concentration. The optimum removal was achieved at pH 6, 20°C after 60 min in the presence of 2.5g/L marble dust. The rates of adsorption were found to follow the pseudo-second-order model. The results showed better fitting to Freundlich isotherm. The thermodynamic studies revealed that the adsorption process is spontaneous, exothermic and favorable at low temperature. The free energy (ΔG°), enthalpy (ΔH°), and entropy (ΔS°) changes were calculated to predict the nature of adsorption. The removal efficiency was improved by calcination of the marble at 700°C. Application for textile wastewater showed high removal efficiency up to 99.9% of inorganic and organic pollutants. The product of treatment was used in the concrete and bricks manufactured, so there is no generation of second-order pollutants.

Keywords: marble dust, pollutant, adsorbent, dye, heavy metals, textile wastewater

1. Introduction

Management of the industrial solid waste and its proper disposal is one of the foremost environmental issues that persist since the industrial revolution (Ngoc and Schnitzer, 2009; Zurbrügg et al., 2012; Tunc, 2019). It has been estimated that around 20 - 25% of the total weight of the produced marble turn into fine waste (Danish et al., 2021). The quantity of produced marble waste is considerable and varies between 5 and 6 million tons per year (Danish et al., 2021). The majority of marble waste occurs during the cutting and polishing processes (Singhal et al., 2021). The improper and random disposal of these huge quantities of waste poses a serious threat to the environment in many respects. It makes fertile land impervious, polluting rivers and other waterways. Also, it causes serious polluting the air as dust clouds after drying, which has a negative impact on irrigation and drinking water resources (Danish et al., 2021). Therefore, it is necessary to find a safe solution to get rid of this waste, and it is preferable to use it in useful applications.

Significant dangerous chemicals are being released into the environment as industrial effluents (Habiba et al., 2019; Thasneema et al., 2021). Also, the emissions of harmful textile dyes and non-biodegradable, heavy metals such as arsenic, chromium, cadmium, copper, zinc, lead, and mercury are worries for the environment and the economy (Tchounwou et al., 2012; Yin et al., 2018). They are a subject of growing worry due to their toxicity, persistence, and accumulate in human bodies and other living organisms, which has a negative impact on health. The removal of many dyes from aqueous solution such as methylene blue, Direct Red 80, reactive red 123, Direct Red 28, Malachite Green, Reactive Yellow 205 and Acid Blue 25 were investigated (Halimoon and Yin, 2010; Ferreira et al., 2014;

Gunatilake, 2015; Abdel-Shafy, 2015; Abdel-Khalek et al., 2017; Zhang et al., 2020; Velusamy et al., 2021). Thus, the removal of these pollutants is a challenge (Jaishankar et al., 2014; Zhang et al., 2020).

Most of the suggested techniques are either very expensive or inefficient (Santhy and Selvapathy, 2006; Yang and Qiu, 2010; El-Sayed and Abdulhady, 2015; El-Shamy et al., 2017; Khulbe and Matsuura, 2018). Recent researches have focused on the discovery of environmentally friendly, ecological and sustainable approaches and technologies for the treatment of industrial wastewater from heavy metals and dyes (El-maguana et al., 2019; Elgarahy, et al., 2020; Elwakeel, et al., 2020; Farrokhzadeh et al., 2020; Pohl, 2020; Dutta et al., 2021; Elwakeel, et al., 2021; Mashabi, et al., 2022). The simple physical-sorption technique is the most useful and cost effective for heavy metal removal and dyes. Active charcoal is conventionally applied as adsorbent. Although, it is industrial widespread treating wastewater, it remained as high-priced sorbent. Nowadays, agriculture's waste-derived products are used as new sorbents for wastewater processing owing to their secure and financial impacts. These sorbents include chitosan, sunflower stalk, shale oil ash, orange peel, natural clay, soy meal hull, citrus-peels, sawdust, and eggshells (Hassan et al., 2021).

The marble powder is inorganic adsorbent, which is frequently found in Egypt, China, India, Italy, Spain, and Turkey. It contains calcium carbonate, clay, iron oxides, silica, potassium and sodium salts. It is a low-cost inorganic adsorbent can be used for treatment of heavy metals and dye contaminated waters (Diouri et al., 2014; Wazwaz et al., 2019; Ramos et al., 2021; Saleh et al., 2022). The marble waste powder was used as an adsorbent for copper and fluoride ions from aqueous solution at pH 7 through physical adsorption (Mehta et al., 2016) while phosphate adsorption reached to 94% at pH 2 (Saleh et al., 2022). The removal of red reactive anionic dyes 195 and direct yellow dyes 50 from marble dust has been studied (Diouri et al. 2014). Calcined dust at 950°C demonstrated better performance in removing methylene blue (El-maguana et al., 2019).

In this study, the adsorption properties of raw marble powder (MP) and calcined marble powder (CMP) were evaluated as an economical and efficient green adsorbent for Acid Red-1 dye as anionic dye and lead ions. The novelty of this work is the proper disposal of huge quantities of solid pollutants which causes major environmental problems as water and air pollution. Also, the economic value in finding a natural material for waste water treatment without any chemical treatment. The product of the adsorption process was used in the concrete and bricks manufactured. Thus, the generation of second-order pollutants is successfully prevented.

2. Materials and methods

2.1. Materials

25 kg of representative marble sludge sample was collected from marble factory, Shaque El-Thobaan, Turah, Cairo, Egypt. The sample was dried in the sun, then remix in ball mill. A 1 kg of the dried marble powder was calcined at 700°C in a muffle furnace for 2 h. Acid Red-1 dye (as anionic dye) of analytical grade; 99.9% purity (Sigma-Aldrich), was used for the preparation of synthetic dye solution. Lead nitrate [Pb(NO₃)₂] salt of analytical grade, 99% purity (Sigma-Aldrich) was used for preparation of the synthetic solution Pb²⁺ ions.

2.2. Methods

2.2.1. Measurements

The mineral composition of both raw marble powder and calcined marble powder were determined using BRUKER X-Ray Diffractometer (Germany) Model AXS D8 with Cu-target ($\lambda=1.540 \text{ \AA}$ and $n=1$) at 40 kV potential and 40 A. The diffraction data were recorded for 2θ values between 3° and 80° and the scanning rate was 3° min⁻¹. Complete chemical analysis of the samples was carried out using X-ray fluorescence "Rigaku Super Mini 200". A laser Zeta Meter 'Malvern Instruments Model Zeta Sizer NANO ZS' was used for zeta potential measurements. A 0.05 g of a solid marble dust is placed in 50 ml 10⁻² M KCl solution, and then it is conditioned for 5 min at desired pH. The particles size and surface area were measured using a laser particle size analyzer (Model: BT-2001). Characterization of textile wastewater was carried out according to Standard Methods (Borzooui et al., 2021).

2.2.2. Adsorption Experimentse

Adsorption experiments were conducted using 0.1 g of raw marble powder or calcined powder was mixed with 40 ml of dye or metal ion solution of definite concentration, pH and temperature in 100 ml a round bottom flask. The flask is agitated at 200 rpm for a definite time in thermo-state water bath. Then, the adsorbent is removed using centrifuge at 2000 rpm for 5 min. The lead ions concentration was determined using atomic absorption Perkin Elmer, (Model: AA analyst 200) and UV-Vis spectrophotometer at wavelength 506 nm. The lead ions concentration and dye were determined by atomic absorption Perkin Elmer, (AA analyst 200) and UV-Vis spectro-photometer at wavelength 506 nm. To investigate the mechanism and order of adsorption, the initial concentrations and contact times were varied over wide ranges. The amount of adsorbed metal ions or dye per unit mass of marble, q (mg/g), is determined using the following equation (Farah at et al., 2022):

$$\text{Adsorption capacity "q" (mg/g)} = \frac{(C_i - C_f) \times V}{W} \quad (1)$$

where V is the solution volume in liter, W is the weight of marble (g), and C_i and C_f are the initial and final metal ions or dye concentration (mg/l), respectively.

The percent removal of metal ions or dye was calculated using the following equation (Farahat et al., 2022):

$$\text{Removal efficiency \%} = \frac{C_i - C_f}{C_i} \times 100 \quad (2)$$

where C_i and C_f are the initial and final concentration (mg/l), respectively.

3. Results and discussion

3.1. Characterization of marble dust

3.1.1. Chemical and phase analysis

Fig. 1 shows the main diffraction peak is observed at $2\theta=29.72^\circ$ and other peaks at $2\theta=23.36^\circ$, 39.72° and 47.80° correspond to diffraction of calcite phase (CaCO_3). Also, there are other peaks for SiO_2 , and weak peaks for the other residual components (Farrokhzadeh et al., 2020). The sharp peaks indicating the higher crystallinity of the material. The raw marble dust is composed of 64.3% calcite [CaCO_3] and 26.9% dolomite [$\text{CaMg}(\text{CO}_3)_2$] minerals with 2.7% quartz [SiO_2], 2.5% albite [$\text{NaAlSi}_3\text{O}_8$], 2.6% illite [$\text{KAl}_2\text{Si}_3\text{AlO}_{10}(\text{OH})_2$] and 1% bentonite [$\text{NaAlSiO}(\text{OH})\text{H}_2\text{O}$] minerals. The results confirm the chemical analysis. On the other hand, the intensity of CaCO_3 peak (main peak of calcite phase) was little in Calcined sample showing that calcite phase was significantly transformed to CaO through calcination process. The dolomite mineral is dissociated to calcium carbonate and magnesium oxide. The CaO phase peaks approximately were located at $2\theta = 32^\circ, 37^\circ, 54^\circ, 64^\circ$ and 67° (Shaharaki et al., 2009).

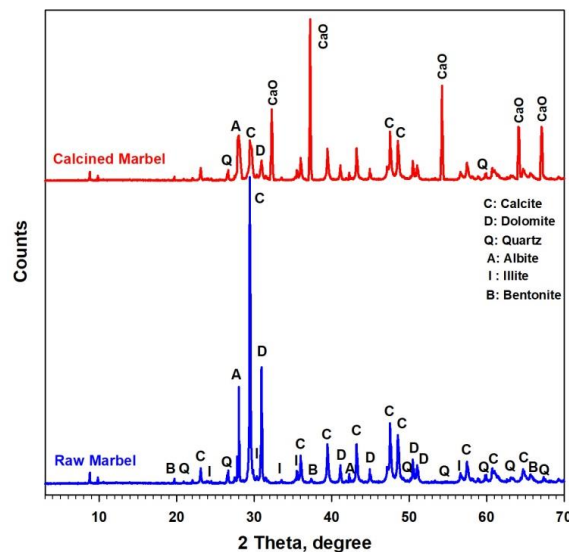


Fig. 1. XRD patterns of the raw and calcined marble dust

Table 1, shows that the sample is composed of 45.5% CaO and 37.6% loss on ignition (LOI) which refers to carbonate dissociation. The sample contains 7.3% as total silica (quartz and silicate). Little amount of other oxides was detected such as MgO, Al₂O₃, Fe₂O₃, TiO₂, Na₂O, K₂O, etc. On the other hand, the calcined marble composed of about 73% CaO and 0.152% LOI which confirmed carbonate dissociation. All other constituents were increased as a result of carbonate dissociation.

Table 1. Complete chemical analysis of the raw and calcined marble dust by XRF

Constituent	SiO ₂	CaO	MgO	Al ₂ O ₃	Fe ₂ O ₃	P ₂ O ₅	SO ₃	Cl ⁻	TiO ₂	Na ₂ O	K ₂ O	L.O.I	Total
Raw MP	7.32	45.52	4.662	2.073	1.553	0.08	0.17	0.035	0.156	0.487	0.285	37.68	100
Calcined MP	11.71	72.99	7.476	3.324	2.490	0.13	0.27	0.056	0.202	0.749	0.457	0.152	100

3.1.2. Zeta-potential measurements

To explain the adsorption mechanisms of metal ions and acid red-1, the zeta potential of raw marble dust and calcined dust were measured as a function of pH, Fig. 2. It is found that the surface of raw dust shows the electronegative behavior in the pH range 4 - 8.41 while the calcine dust shows the same behavior in the pH range 4 - 6.45. The calcined reveals less zetanegative potential value than the raw dust. Thus the point of zero charge (PZC) of the raw and calcined marble was 8.41 and 6.45, respectively. A further increase in the pH value above the PZC, the surface was turned positive. These results reveal high consistency with previous reported zeta potential (Sposito et al., 2021).

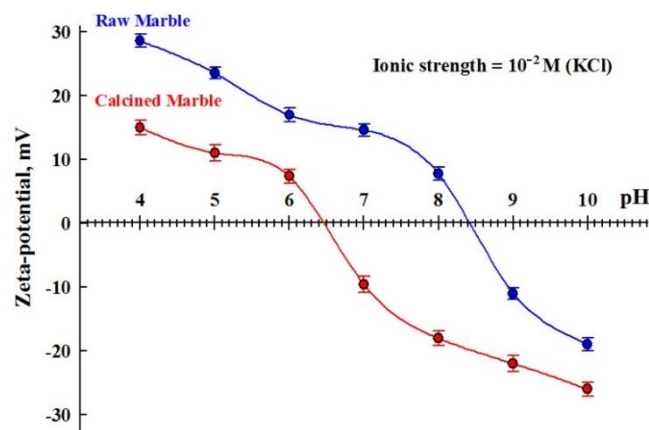


Fig. 2. Zeta-potential of the raw and calcined marble dust as a function of pH.

3.1.3. Particle size and surface area measurements

The particle size distribution is illustrated in Fig. 3. The average particle size (D_{50}) is 6.656 μm and the particle size of the whole sample is less than 57 μm . The average surface area is 483.6 m^2/kg .

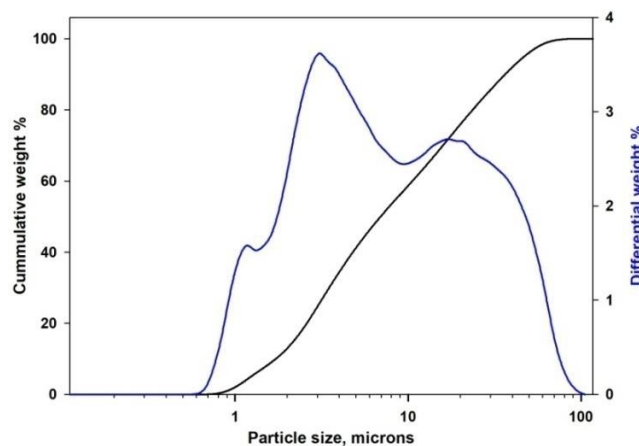


Fig. 3. Particle size distribution of the raw marble dust

3.2. Adsorption of lead ions and acid red dye

3.2.1. Effect of pH

The pH is an important factor affecting the removal efficiency. It may cause dissociation of the adsorbent sites and changes of the solution chemistry of metal ions and dye. It may be distributed the surface charge on the adsorbent surface (Sanad et al., 2021). Fig. 4 indicates that the removal efficiency of lead ions and acid red dye increases with increasing the pH of the solution till reach the maximum value at pH = 6. The maximum removal of the lead ions (53.2%) and acid red dye (57.3%) is achieved at pH = 6. The positive charged marble surface, suggesting high adsorption efficiency with anionic charged dye due to the strong electrostatic interaction. The low attraction of anionic dye in the acidic medium to negative surface can be explained by the protonation of several functional groups which are acting as positively charged species and thus the adsorption of anionic dye is reduced (Abdel-Khalek et al., 2019). Conversely, the attraction of positively charged lead ions to positive surface can be explained by the formation of the negative $Pb(CO_3)_2^{2-}$ species through the reaction of lead ions with released carbonate species (Schock, 1980). On the other hand, the maximum removal was 73.3% and 84.4% for lead ions and acid red dye, respectively at pH = 6. The pH of the aqueous solution was rapidly changed upon addition of calcined marble. This might be due to partial dissolution of alkaline metal oxides in aqueous medium. The high performance of calcined marble is expected due to oxide formation and removal of crystallized water (Shaharaki et al., 2009).

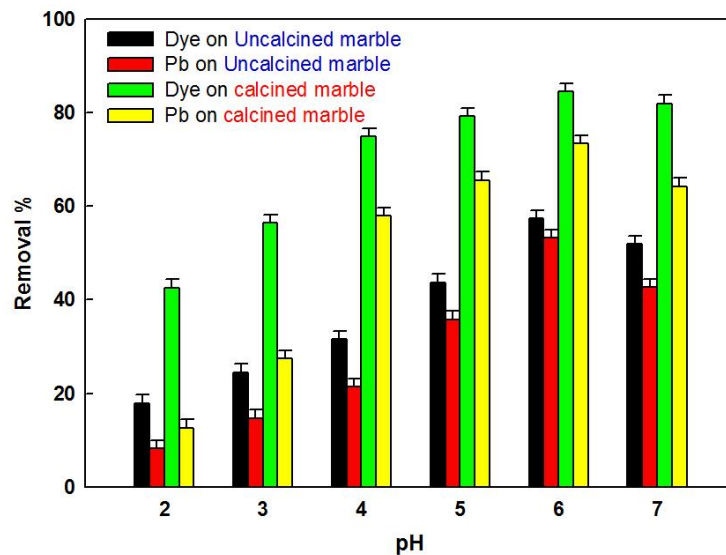


Fig. 4. Effect of pH on the removal efficiency of the raw and calcined marble dust

3.2.2. Effect of contact time

The removal efficiency was studied as a function of contact time, Fig. 5. The removal efficiency was reached to about 60% after 60 min while it reached to about 70% after 240 min. The high adsorption rate in the first 60 min is due to the gradual decrease in the adsorption sites on the marble surface. In case of calcined marble, the removal is reached to about 70% after 60 min while it reached to about 75% after 240 min. The adsorption process is controlled by the amount of lead ions or dye molecules transported from the bulk liquid phase to the marble surface. So, the adsorption increased with time until saturation (Mahmoud et al., 2019). The calcined marble exhibited an adsorption capacity of 93 and about 95 mg/g for lead ions and acid red dye, respectively at 20°C and pH 6 after 240 min. It indicates that the sorption capacity was good with comparing to literature (98 mg/g and 14 mg/g for Acid Red dye and lead ions) (Abbad and Alakhras, 2020; Rakhym et al., 2020).

3.2.3. Effect of initial concentration

Fig. 6 shows the sorption performance of marble as a function of concentration. The increasing of the initial concentration led to an increase of adsorption capacity and a decrease of removal efficiency.

High concentration of lead or dye indicates that more lead ions or dye molecules are available. Therefore, each unit mass of the marble powder exposes to a larger number of lead ions or dye molecules, which gradually filling up the sites. The adsorption was running till reach saturation causing the decrease in the removal efficiency. The raw and calcined marble exhibited the maximum adsorption capacities of about 60 and 80 mg/g from 200 ppm of the lead ions or acid red dye, respectively at 20°C and pH 6 after 30 min.

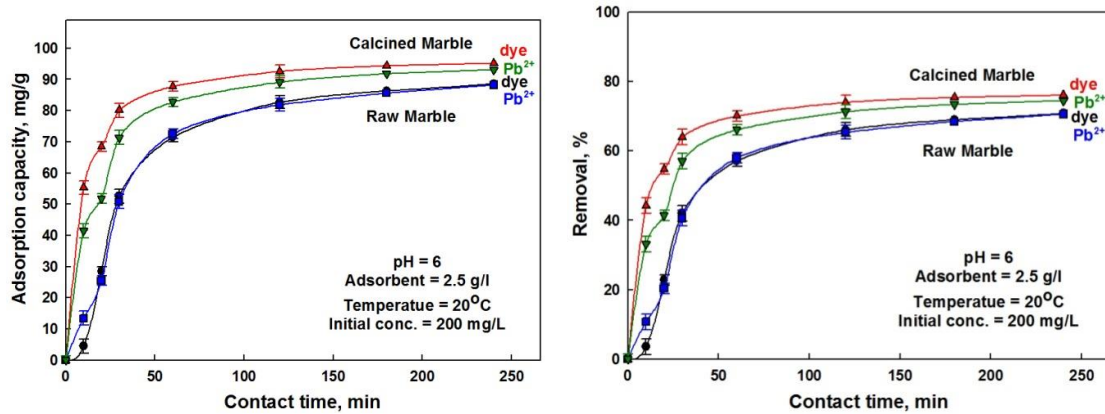


Fig. 5. Effect of contact time on ads. capacity and removal % of the raw and calcined marble dust

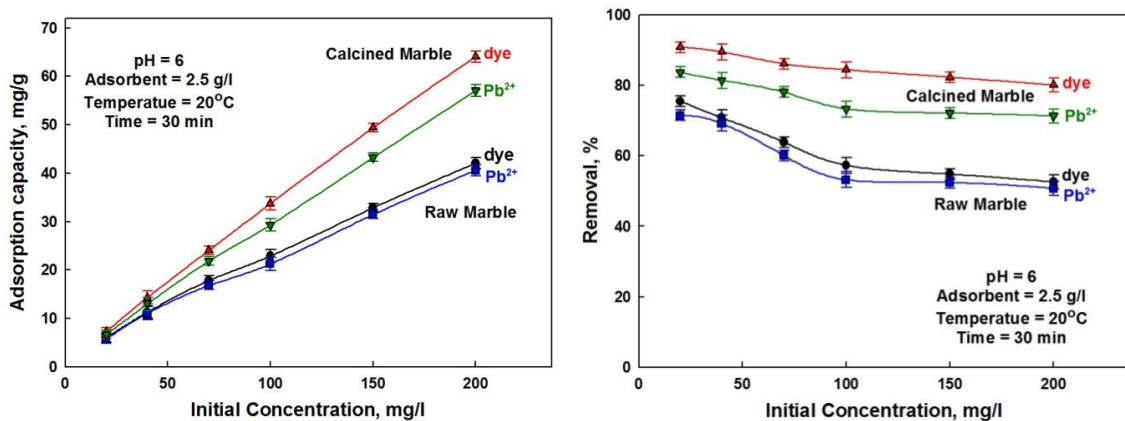


Fig. 6. Effect of initial concentration on ads. capacity and removal % of the raw and calcined marble

3.2.4. Effect of temperature

Fig. 7 shows the sorption performance of marble as a function of temperature. Although, it is known that the adsorption process is induced by increasing the temperature, but in this case the adsorption is reduced at higher temperature (Mahmoud et al., 2019). The sorption capacity decreased by increasing the temperature from 20°C to 60°C, the maximum sorption of lead ions and acid red dye was at 20°C. A decrease in the sorption capacity with rising temperature may be due to the damage of active sorption sites of the marble surface. It may be due to increasing the tendency to desorb species from the interface to the solution. These results suggest the exothermic nature of the sorption process onto the surface of raw and calcined marble dust (Abdel-Khalek et al., 2019).

3.2.5. Effect of adsorbent amount

Fig. 8 shows the effect of adsorbent amount on the sorption capacity onto marble dust. The adsorption capacity decreased as the adsorbent dosage increased because the adsorption sites on the adsorbent surface were not fully utilized at a higher adsorbent dosage in comparison with the lower adsorbent dosage (Ho and McKay, 2000). On the other hand, the removal efficiency, increased as the sorbent dosage increased due to the number of active sites available for adsorption increased, leading to an increase in the removal percentage (Ismail et al., 2014). In practice, higher removal efficiency of up to 27% is suggested to use a higher dosage due to the economic adsorbent.

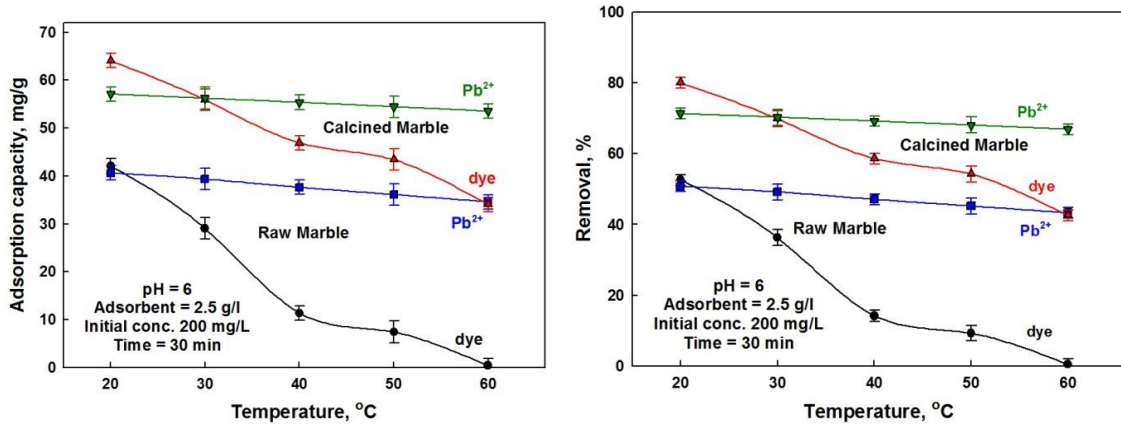


Fig. 7. Effect of temperature on ads. capacity and removal% of the raw and calcined marble dust.

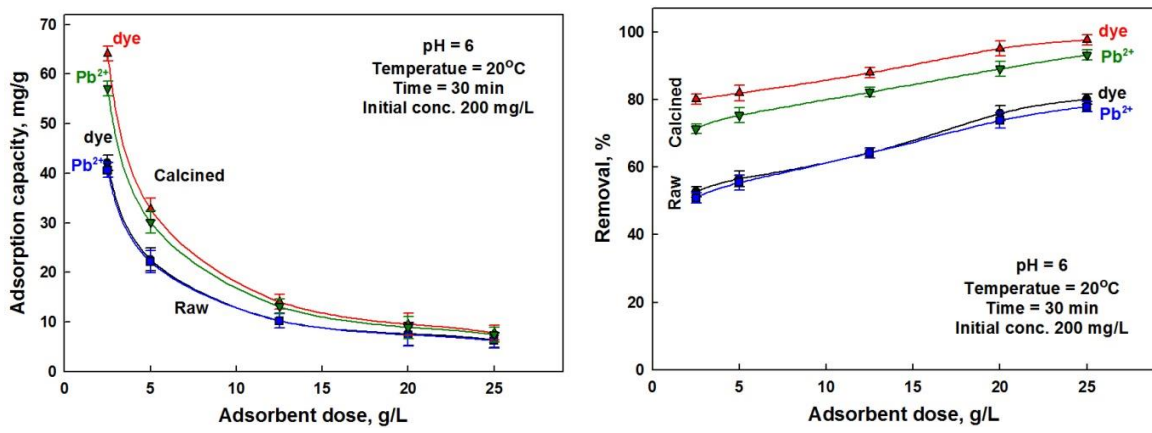


Fig. 8. Effect of adsorbent dose on ads. capacity and removal% of the raw and calcined marble dust.

3.2.6. Adsorption isotherms

The adsorption isotherms are used to analyze the interaction mechanism between the adsorbate species and adsorbent surface (Wang et al., 2006). Thereby, the Langmuir and Freundlich isotherms are implemented to explore the adsorption process. So, Temkin, Langmuir and Freundlich isotherms are applied to explore the sorption process.

Temkin isotherm is expressed as:

$$1. \quad q_t = B \ln A_T + B \ln C_f \quad (3)$$

where, C_f (mg/l) is the final concentration, q_t (mg/g) is the adsorbed amount at time t , B (mg/g) (maximum adsorption) is monolayer adsorption capacity and A_T (L/mg) is a binding constant related to the free energy of adsorption.

Langmuir Isotherm is expressed as:

$$\frac{C_f}{q_t} = \frac{C_f}{q_{max}} + \frac{1}{b q_{max}} \quad (4)$$

where, C_f (mg/l) is the final concentration, q_t (mg/g) is the adsorbed amount at time t , q_{max} (mg/g) (maximum adsorption) is monolayer adsorption capacity and b (L/mg) is a binding constant related to the free energy of adsorption. Freundlich Isotherm is expressed as:

$$\ln q_t = \ln k + \frac{1}{n} \ln C_f \quad (5)$$

where, q_t (mg/g) is the adsorbed amount, C_f (mg/L) is the final concentration, K is the indicative of the extent of the adsorption and n is the adsorption intensity.

The adsorption isotherms are shown in Fig. 9 (a-c). The isotherm model parameters were evaluated based on the correlation coefficient (R^2), Table 2. The Freundlich model provided the best linearity for all systems. This means that the sorption is characterized mainly by physical nature that may occur by electrostatic interaction of the opposite charge. The Langmuir model provided good linearity for dye

sorption. The predicted equilibrium sorption values using Langmuir isotherm came close to the experimental value of the dye, but far from the value of the lead. This means that there some extent of the chemical nature of the dye sorption. On the other hand, the heterogeneity factor of “n” is a measure of the favorability of sorption and the degree of heterogeneity of adsorbate on the adsorbent surface. The value of n is higher than 1, suggesting a favorable adsorption of red dye and lead ions on the raw and calcined marble waste powder (Visa, 2016).

Table 2. The parameters of Temkin, Langmuir and Freundlich isotherm models

Isotherm	Parameters	Raw marble		Calcined marble	
		Red dye	Lead	Red dye	Lead
Temkin	R ²	0.8956	0.8906	0.8921	0.8932
	B	11.5321	11.3417	17.8996	16.5531
	A _T	0.2524	0.2201	0.5823	0.3305
Langmuir	R ²	0.9491	0.8586	0.9597	0.8765
	q _{max} (Cal.)	59	99	70	98
	q _{max} (Exp.)	42	40	64	57
	b	0.01849	0.00936	0.05204	0.01934
Freundlich	R ²	0.9965	0.9945	0.9982	0.9966
	n	1.569	1.530	1.428	1.375
	K _F	2.246	1.926	4.946	2.904

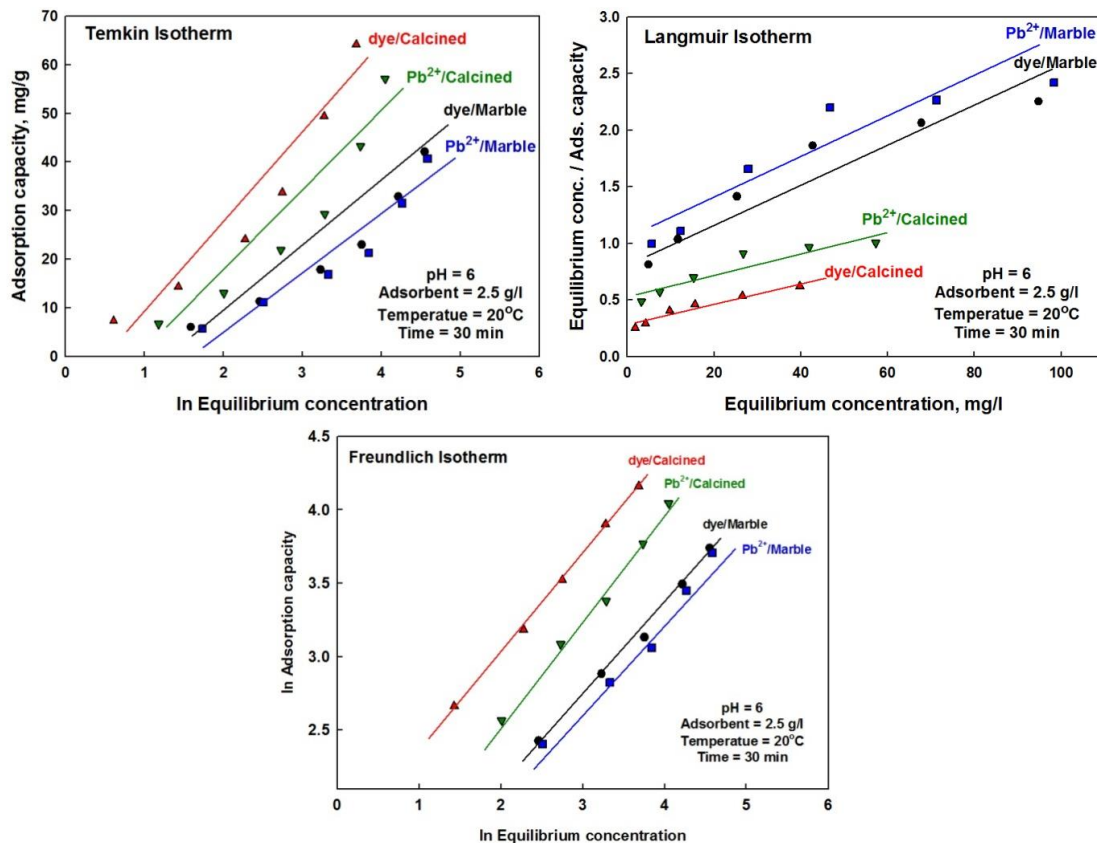


Fig. 9. Plot of Temkin (A), Langmuir (B) and Freundlich (C) isotherm models

3.2.7. Adsorption kinetics

The sorption kinetics is investigated at various contact times up to 240 min. The initial concentration of lead ions and dye was fixed at 200 mg/L. Two kinetic models were investigated, namely pseudo first-

order (Aklan et al., 2008) and pseudo-second order (Duan et al., 2016). Their linear equations are presented as:

$$\text{The pseudo-first-order equation: } \ln q_e - q_t = \ln q_e - k_1 t \quad (6)$$

$$\text{The pseudo-second-order equation: } \frac{t}{q_t} = \frac{1}{k_2 q_e^2} - \frac{t}{q_e} \quad (7)$$

where, q_t and q_e (the ions adsorbed at time t and at equilibrium) and k_1 and k_2 (the rate constants of the first-order and second-order reactions).

Although, the linear regression coefficients (R^2) were 0.96 – 0.97 of plotting $\log(q_e - q_t)$ versus time, according to pseudo-first-order kinetic model, the predicted equilibrium adsorption was lower than the experimental results. It indicates that the pseudo first-order kinetics cannot be applied, Fig. 10 (a & b) and Table 4. The higher values of regression coefficient (R^2) for plotting of t/q with time indicated that the pseudo-second-order model is better in describing the adsorption kinetics. Moreover pseudo-second-order kinetic model predicts a closer value of the adsorption compared with the experimental results. Hence, it confirms the suitability of applying this model. It investigates kinetic behavior in the case of a chemical reaction being the rate controlling step (chemical sorption).

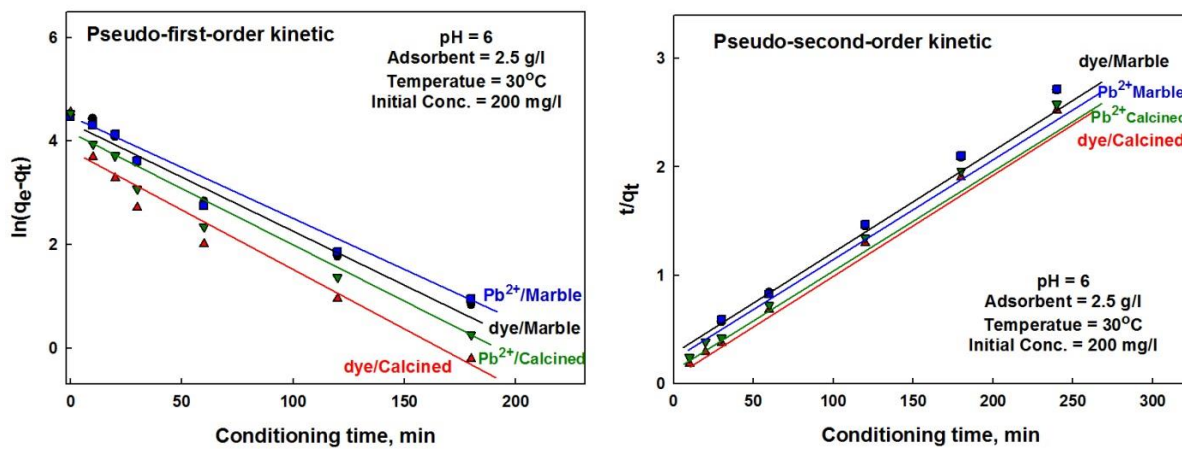


Fig. 10. Plot of the pseudo-first-order and pseudo-second-order kinetic models.

Table 4. The parameters of the pseudo-first-order and pseudo-second-order kinetic models.

Kinetic model	Parameters	Raw marble dust		Calcined marble	
		Red dye	Lead	Red dye	Lead
Pseudo-first-order	R^2	0.9782	0.9724	0.9441	0.9619
	K_1	2.1×10^{-2}	2.0×10^{-2}	2.4×10^{-2}	2.2×10^{-2}
	Calculated q_e	81.6	78.4	47.8	60.1
	Experimental q_e	88.6	88.2	95.1	93.1
Pseudo-second-order	R^2	0.9996	0.9991	0.9999	0.9999
	K_2	4.34×10^{-4}	4.31×10^{-4}	1.49×10^{-3}	9.57×10^{-4}
	Calculated q_e	93.4	92.7	98.0	97.0
	Experimental q_e	88.6	88.2	95.1	93.1

The particle diffusion model is based on the assumption that the rate limiting step may be a chemical adsorption involving the valence forces through the sharing or exchange of electrons between the adsorbent and the adsorbate. In most adsorption processes, the uptake varies almost proportionately with $t^{0.5}$ rather than with the contact time and can be represented as follows:

$$q_t = k_{id} t^{0.5} + I \quad (8)$$

where q_t is the amount adsorbed at time t and $t^{0.5}$ is the square root of the time and K_{id} ($\text{mg g}^{-1} \text{min}^{-0.5}$) is the rate constant of intra-particle diffusion and I is the intercept. The values of I give information about the thickness of the boundary layer, i.e. the larger intercept the greater is the boundary layer effect, Table 5.

Table 5. The parameters of the particle diffusion model

Particle diffusion model							
"l" Thickness of the boundary layer				Rate constant of intra-particle diffusion			
Raw marble dust		Calcined marble		Raw marble dust		Calcined marble	
dye	Pb ²⁺	dye	Pb ²⁺	dye	Pb ²⁺	dye	Pb ²⁺
3.3330	5.1339	33.6053	23.7417	6.3897	6.2093	5.0182	5.4597

3.2.8. Thermodynamic study

The spontaneity of the sorption process can be investigated through thermodynamics parameters such as enthalpy (ΔH), entropy (ΔS), and Gibb's free energy (ΔG). They were determined from the slope and intercept of the straight line of the plot $\ln K_c$ versus $1/T$, Fig. 11, through Van't Hoff equation (Abdi et al., 2017):

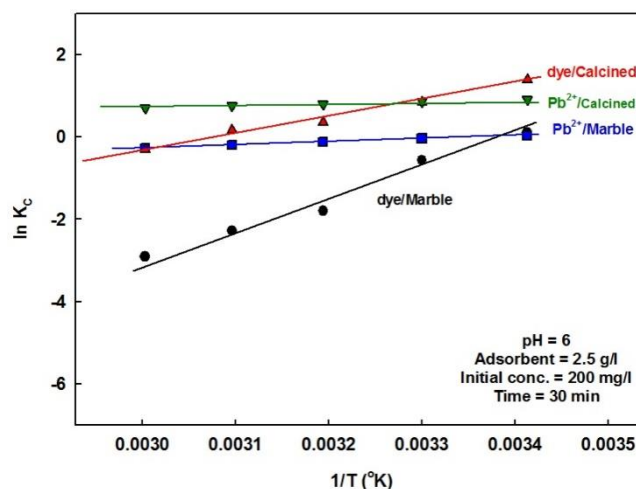
$$\ln K_c = \frac{\Delta S^\circ}{R} - \frac{\Delta H^\circ}{RT} \quad (9)$$

where: T is the temperature in kelvin, and R is the gas constant [8.314 J/mol K]. The $k_c = (f/1-f)$, where f is the removal fraction.

The standard Gibbs free energy change ΔG° is estimated using the following equation (Li et al., 2019):

$$\Delta G^\circ = -RT \ln K_c \quad (10)$$

It is found that the mean free energy values of the sorption systems increase with rising temperature from 20 to 60°C and they turned from negative to positive values for most systems. The negative ΔG° is meaning the spontaneous behavior of the sorption process. Thus, the increase of ΔG° with increasing temperature reveals that the adsorption process is being less favorable at high temperature.

Fig. 11. Plot of $\ln K_c$ versus $1/T$

The negative ΔH° values suggest the exothermic nature of the sorption system, Table 6. The higher ΔH° values confirms the chemisorption process as reflected in the Langmuir isotherm for acid red dye. The lower ΔH° values for lead confirms the physical adsorption, as shown by the Freundlich isotherm. Furthermore, the negative ΔS° indicates the decreasing of a random degree at the interface layer between solid and liquid during the adsorption, suggesting the adsorption is less favorable at higher temperature.

3.3. Application for textile wastewater

The marble dust was employed for a textile wastewater treatment. Two cycle were carried out using 5g of marble dust in one liter of the textile wastewater at pH = 6 and 20°C for 60 min. The removal efficiency of the first cycle was 75 - 95%, while it was 94 - 99% for all inorganic and organic pollutants after the second cycle, Table 7. The values in the last column of Table 7 are the International Standard

for Drinking Water (UNICEF, 2017). It is clear that, the treated wastewater of the first cycle doesn't meet the International Standard for Drinking water but can be recycled. The second cycle produced a good water that meets the International Standard for Drinking Water. The recoverability of the marble waste in the adsorption was not investigated because it can't be treated with acidic. Moreover, the marble waste is cheap. The product could be applied to make artificial bricks and marble which will be discussed in another study. Thus, the generation of second-order pollutants is successfully prevented.

Table 6. Thermodynamic parameters of sorption systems

Temp. °C	Raw marble dust						Calcined marble dust					
	Red dye			Lead			Red dye			Lead		
	ΔH°	ΔS°	ΔG°	ΔH°	ΔS°	ΔG°	ΔH°	ΔS°	ΔG°	ΔH°	ΔS°	ΔG°
	KJ.mol ⁻¹	J.k ⁻¹	J.k ⁻¹ .mol ⁻¹	KJ.mol ⁻¹	J.k ⁻¹	J.k ⁻¹ .mol ⁻¹	KJ.mol ⁻¹	J.k ⁻¹	J.k ⁻¹ .mol ⁻¹	KJ.mol ⁻¹	J.k ⁻¹	J.k ⁻¹ .mol ⁻¹
20			-253			-78			-3392			-2223
30			1411			81			-2128			-2171
40	-98.9	-332	4680	-6.2	-21	307	-33.0	-102	-909	-4.2	-6.8	-2106
50			6116			522			-462			-2037
60			14389			752			825			-1948

Table 7. Evaluation of the textile wastewater and treated water to meet International Standard for Drinking Water

Composition mg/l	Raw Textile wastewater	Treated Cycle 1	Treated Cycle 2	Total Removal %	Standard limits
pH	10	7.4	7.2	---	7.0-8.5
TS ¹	247	35.4	6.281	97.4	500
Cl	75	17.2	3.184	95.7	200
Sulfate	148	29.6	5.723	96.1	200
COD ²	684	42.9	9.168	98.6	10
Nitrate	24	5.23	1.157	95.2	10
Turbidity	276	59.4	1.247	99.5	5.0
Zn	18.47	4.027	0.918	95.0	5.0
BOD ³	9.613	2.935	0.372	96.1	2.0
Cu	15.94	3.425	0.825	94.8	1.0
Cr	3.373	0.813	0.159	95.2	0.50
Ni	5.589	1.236	0.234	95.8	0.50
As	3.176	0.773	0.176	94.4	0.20
Pb	3.432	0.804	0.187	94.5	0.10
Cd	0.581	0.124	0.029	95.0	0.05
TOC ⁴	75.31	3.96	0.237	99.6	0.30
Sulfide	83.53	3.817	0.041	99.9	0.05
Color %	39	6.2	1.36	96.5	15

¹Total Solids ²Chemical Oxygen Demand ³Biochemical oxygen demand ⁴Total Organic Carbon

4. Conclusions

The marble dust waste and its calcined form were successfully used as an economical adsorbent for industrial wastewater treatment. The raw marble is mainly composed of calcite and dolomite minerals with little amount of quartz, illite, albite and bentonite minerals. The calcite and dolomite minerals were dissociated to oxides by calcination. The point of zero charge (PZC) was 8.41 and 6.45 for raw and calcined marble dust, respectively. The average particle size (D_{50}) is 6.656 μm with an average surface area is 483.6 m^2/kg .

The removal efficiency for synthetic lead ions and acid red dye solutions at different pH, temperature, contact time, adsorbent dose and initial concentration showed that the maximum efficiency is achieved at pH 6 and 20°C. The Freundlich model provided the best linearity for all systems, suggesting physical adsorption. The Langmuir model provided good linearity for dye sorption suggesting some extent of the chemical nature of the dye sorption. The pseudo-second-order model is better in describing the adsorption kinetics. The negative ΔH° values suggest the exothermic nature of the sorption system while the negative ΔS° indicates the decreasing of a random degree at the interface layer between solid and liquid. The free energy indicated that the spontaneous behavior of the sorption process at low temperature.

The marble dust was employed for textile wastewater treatment at optimum parameters. The removal efficiency of the second cycle was 94–99.9% for all types of the pollutants. The treated water meets the International Standard for Drinking water. The residue of the treatment process could be used in the concrete and bricks manufactured.

References

- ABBAD, E., ALAKHRAS, F., 2020. *Removal of Dye Acid Red 1 from Aqueous Solutions Using Chitosan-iso-Vanillin Sorbent Material*. Indonesian J. of Sci. & Tech., 5, 3, 352-365.
- ABDEL-KHALEK, M.A., ABDEL-RAHMAN, M.K., FRANCIS, A.A., 2017. *Exploring the adsorption behavior of cationic and anionic dyes on industrial waste shells of egg*, Journal of Environmental Chemical Engineering, 5, 319-327.
- ABDEL-KHALEK, M.A., MAHMOUD, G.A., SHOUKRY, E.M., AMIN, M., ABDUL-GHAHANY, A.H., 2019. *Adsorptive removal of nitrate ions from aqueous solution using modified biodegradable-based hydrogel*, Desalination & Water Treatment, 155, 390-401.
- ABDEL-SHAIFY, H.I., 2015. *Chemical treatment for removal of heavy metals from industrial wastewater*. Egyptian Journal of Chemistry, 58, 1, 1-12.
- ABDI, J., VOSSOUGH, M., MAHMOUDI, N., ALEMZADEH, I., 2017. *Synthesis of metal-organic framework hybrid nanocomposites based on GO and CNT with high adsorption capacity for dye removal*, Chem. Eng. J. 326, 1145-1158.
- ALKAN, M., DOGAN, M., TURAN, Y., DEMIRBAS, O., TURAN, P., 2008. *Adsorption kinetics and mechanism of maxilon blue 5G dye on sepiolite from aqueous solutions*, Chem. Eng. J. 139, 213-223.
- BORZOOEI, S., SIMONETTI, M., SCIBILIA, G., ZANETTI, M.C., 2021. *Critical evaluation of respirometric and physicochemical methods for characterization of municipal wastewater during wet-weather events*, Journal of Environmental Chemical Engineering, 9, 3, 105238.
- DANISH, A., MOSABERPANAH, M.A., SALIM, M.U., FEDIUK, R., RASHID, M.F., WAQAS, R.M., 2021. *Reusing marble and granite dust as cement replacement in cementitious composites: A review on sustainability benefits and critical challenges*. Journal of Building Engineering, 44, 102600.
- DIOURI, K., CHAQRONE, A., KHERBECH, A., MIYAH, Y., LAHRICHI, A., 2014. *Kinetics of Direct Yellow 50 dye adsorption onto marble powder sorbents*. International Journal of Innovative Research in Science Engineering and Technology, 3, 16626.
- DUAN, P., YAN, C., ZHOU, W., REN, D., 2016. *Development of fly ash and iron ore tailing based porous geopolymer for removal of Cu(II) from wastewater*, Ceram. Int. 42, 12, 13507-13518.
- DUTTA, S., GUPTA, B., SRIVASTAVA, S.K., GUPTA, A.K., 2021. *Recent advances on the removal of dyes from wastewater using various adsorbents: A critical review*. Materials Advances., 2, 4497-4531.
- ELGARAHY, A.M., ELWAKEEL, K.Z., MOHAMMED, S.H., ELSHOUBAKY, G.A., 2020. *Multifunctional eco-friendly sorbent based on marine brown algae and bivalve shells for subsequent uptake of Congo red dye and copper(II) ions*, Journal of Environmental Chemical Engineering, 8, 4, 103915.
- EL-MAGUANA, Y., ELHADIRI, N., BOUCHDOUG, M., BENCHANAA, M., 2019. *Valorization of powdered marble as an adsorbent for removal of methylene blue using response surface methodology*. Applied Journal of Environmental Engineering Science, 5, 1, 53-65.
- EL-SAYED, M.H., ABDELHADY, Y.A., 2015. *Heavy metals removal by using magnetic iron oxide/TiO₂ nanocomposite for wastewater treatment in 10th of Ramadan city, Egypt*. Egyptian Journal of Desert Research, 65, 1, 81-99.

- EL-SHAMY, A.M., FARAG, H.K., SAAD, W., 2017. *Comparative study of removal of heavy metals from industrial wastewater using clay and activated carbon in batch and continuous flow systems*. Egyptian Journal of Chemistry, 60, 6, 1165-1175.
- ELWAKEEL, K.Z., ELGARAHY, A.M., GUIBAL, E., 2021. *A biogenic tunable sorbent produced from upcycling of aquatic biota-based materials functionalized with methylene blue dye for the removal of chromium(VI) ions*, Journal of Environmental Chemical Engineering, 9, 2, 104767.
- ELWAKEEL, K.Z., ELGARAHY, A.M., KHAN, Z.A., ALMUGHAMISI, M.S., AL-BOGAMI, A.S., 2020. *Perspectives regarding metal/mineral-incorporating materials for water purification: with special focus on Cr(vi) removal*, JF - Materials Advances, 1, 6, 1546-1574.
- FARAHAT, M.M., Abdel-Khalek, M.A., SANAD, M.S., 2022. *Affordable and reliable cationic-anionic magnetic adsorbent: Processing, characterization, and heavy metals removal*, Journal of Cleaner Production, 360, 132178, ISSN 0959-6526.
- FARROKHZADEH, S., RAZMI, H., JANNAT, B., 2020. *Study of Reactive Red 195 anionic dye adsorption on calcined marble powder as potential eco-friendly adsorbent*. Human, Health and Halal Metrics, 1, 1, 42-56.
- FERREIRA, A.M., COUTINHO, J.A., FERNANDES, A.M., FREIRE, M.G., 2014. *Complete removal of textile dyes from aqueous media using ionic-liquid-based aqueous two-phase systems*. Separation and Purification Technology, 128, 58-66.
- GUNATILAKE, S.K., 2015. *Methods of removing heavy metals from industrial wastewater*. Methods, 1, 1, 14.
- HABILA, M.A., AL-OTHTMAN, Z.A., GHFAR, A.A., AL-ZABEN, M.I., AL-OTHTMAN, A.A., ABDELTAWAB, A. A., SHEIKH, M., 2019. *Phosphonium-based ionic liquid modified activated carbon from mixed recyclable waste for mercury (II) uptake*. Molecules, 24, 3, 570.
- HALIMOON, N., YIN, R.G.S., 2010. *Removal of heavy metals from textile wastewater using zeolite*. Environment Asia, 3, 124-130.
- HASSAN, E.R., ROSTOM, M., FARGHALY, F.E., ABDEL-KHALEK, M.A., 2021. *Bio-sorption for tannery effluent treatment using eggshell wastes; kinetics, isotherm and thermodynamic study*, Egyptian Journal of Petroleum, 29, 4, 273-278.
- HO, Y.S., MCKAY, G., 2000. *The Kinetics of Sorption of Divalent Metal Ions Onto Sphagnum Moss Peat*. Water Research-Water Res., 34, 735-742.
- ISMAIL, L.F., SALLAM, H.B., ABOFARHA, S.A., GAMAL, A.M., MAHMOUD, G.E., 2014. *Adsorption behaviour of direct yellow 50 onto cotton fiber: equilibrium, kinetic and thermodynamic profile*. Spectrochim Acta A Mol Biomol Spectrosc. 15, 131, 657-66.
- JAISHANKAR, M., TSETEN, T., ANBALAGAN, N., MATHEW, B.B., BEEREGOWDA, K.N., 2014. *Toxicity, mechanism and health effects of some heavy metals*. Interdisciplinary toxicology, 7, 2, 60.
- KHULBE, K.C., MATSUURA, T., 2018. *Removal of heavy metals and pollutants by membrane adsorption techniques*. Applied water science, 8, 1, 1-30.
- LI, Y., LU, H., WANG, Y., ZHAO, Y., LI, X., 2019. *Efficient removal of methyl blue from aqueous solution by using poly(4-vinylpyridine)-graphene oxide-Fe₃O₄ magnetic nanocomposites*, J. Mater. Sci. 54, 7603-7616.
- MAHMOUD, G., ABDEL-KHALEK, M., SHOUKRY, E., AMIN, M., ABDULGHANY, A., 2019. *Removal of Phosphate Ions from Wastewater by Treated Hydrogel Based on Chitosan*. Egyptian Journal of Chemistry, 62, 8, 1537-1549.
- MASHABI, R.A., KHAN, Z.A., ELWAKEEL, K.Z., 2022. *Chitosan- or glycidyl methacrylate-based adsorbents for the removal of dyes from aqueous solutions: a review*, Materials Advances, 3, 14, 5645-5671.
- MEHTA, D., MONDAL, P., GEORGE, S., 2016. *Utilization of marble waste powder as a novel adsorbent for removal of fluoride ions from aqueous solution* Dhiraj Mehta, Poonam Mondal, Suja George Journal of Environmental Chemical Engineering 4, 932-942.
- NGOC, U.N., SCHNITZER, H., 2009. *Sustainable solutions for solid waste management in Southeast Asian countries*. Waste management, 29, 6, 1982-1995.
- POHL, A., 2020. *Removal of heavy metal ions from water and wastewaters by sulfur-containing precipitation agents*. Water, Air & Soil Pollution, 231, 10, 1-17.

- RAKHYM, A.B., SEILKANOYA, G.A., KURMANBAYEVA, T.S., 2020. *Adsorption of lead ions from water solutions with natural zeolite and chamotte clay*, *Materials Today: Proceedings*, 31, 3, 482-485, <https://doi.org/10.1016/j.matpr.2020.05.672>.
- RAMOS, V.C., UTRILLA, J.R., SANCHEZ, A.R., RAMON, M.V.L., POLO, M.S., 2021. *Marble Waste Sludges as Effective Nanomaterials for Cu(II) Adsorption in Aqueous Media*. *Nanomaterials*, 11, 9, 2305.
- SALEH, M., ISIK, Z., ARSLAN, H., YALVAC, M., DIZGE, N., 2022. *Adsorption of Phosphate Ions from Aqueous Solutions using Marble, Pumice, and Basalt Triple Combination*. *Water, Air, & Soil Pollution*, 233, 6, 1-16.
- SANAD, M.M.S., FARAHAT, M.A., ABDEL-KHALEK, M.A., 2021. *One-step processing of low-cost and superb natural magnetic adsorbent: kinetics and thermodynamics investigation for dye removal from textile wastewater*, *Advanced Powder Tech.*, 32, 5, 1573-1583.
- SANTHY, K., SELVAPATHY, P., 2006. *Removal of reactive dyes from wastewater by adsorption on coir pith activated carbon*. *Bioresource technology*, 97, 11, 1329-1336.
- SCHOCK, M.R., 1980. *Response of lead solubility to dissolved carbonate in drinking water*. *Journal of American Water Works Association*, 72, 12, 695-704.
- SHAHRAKI, B.K., MEHRABI, B., DABIRI, R., 2009. *Thermal behavior of Zefreh dolomite mine mal behavior of Zefreh dolomite mine (Central Iran)*, *J. Min. Metall. Sect. B Metall.* 45, 35-44.
- SINGHAL, V., NAGAR, R., AGRAWAL, V., 2021. *Use of marble slurry powder and fly ash to obtain sustainable concrete*. *Materials Today: Proceedings*, 44, 4387-4392.
- SPOSITO, R., MAIER, M., BEUNTNER, N., THIENEL, K., 2021. *Evaluation of zeta potential of calcined clays and time-dependent flow-ability of blended cements with customize polycarboxylate-based superplasticizers*, *Construction and Building Materials*, 308, 125061.
- TCHOUNWOU, P.B., YEDJOU, C.G., PATLOLLA, A.K., SUTTON, D.J., 2012. *Heavy metal toxicity and the environment*. *Molecular, clinical and environmental toxicology*, 133-164.
- THASNEEMA, K.K., DIPIN, T., THAYYIL, M.S., SAHU, P.K., MESSALI, M., ROSALIN, T., HADDA, T. B., 2021. *Removal of toxic heavy metals, phenolic compounds and textile dyes from industrial waste water using phosphonium based ionic liquids*. *Journal of Molecular Liquids*, 323, 114645.
- TUNC, E.T., 2019. *Recycling of marble waste: A review based on strength of concrete containing marble waste*. *Journal of environmental management*, 231, 86-97.
- UNICEF, 2017. *Thematic Report on drinking water*, *World Health Organization*, Avenue Appia 20 1211 Geneva 27, Switzerland. <https://apps.who.int/iris/handle/10665/325897>.
- VELUSAMY, S., ROY, A., SUNDARAM, S., KUMAR MALLICK, T., 2021. *A review on heavy metal ions and containing dyes removal through graphene oxide-based adsorption strategies for textile wastewater treatment*. *The Chemical Record*, 21, 7, 1570-1610.
- VISA, M., 2016. *Synthesis and characterization of new zeolite materials obtained from fly ash for heavy metals removal in advanced wastewater treatment*, *Powder Technol.* 294, 338-347.
- WANG, S., SOUDI, M., LI, L., ZHU, Z., 2006. *Coal ash conversion into effective adsorbents for removal of heavy metals and dyes from wastewater*, *J. Hazard.Mater.* 133, 243-251.
- WAZWAZ, A., AL-SALAYMEH, A., KHAN, M.S., 2019. *Removing heavy metals through different types of soils and marble powder found in Oman*. *Journal of Ecological Engineering*, 20, 4.
- YANG, J., QIU, K., 2010. *Preparation of activated carbons from walnut shells via vacuum chemical activation and their application for methylene blue removal*. *Chemical Engineering Journal*, 165, 1, 209-217.
- YIN, J., DENG, C., YU, Z., WANG, X., XU, G., 2018. *Effective removal of lead ions from aqueous solution using nano illite/smectite clay: isotherm, kinetic, and thermodynamic modeling of adsorption*. *Water*, 10, 2, 210.
- ZHANG, X., YAN, S., CHEN, J., TYAGI, R.D., LI, J., 2020. *Physical, chemical, and biological impact of hospital wastewater on environment: presence of pharmaceuticals, pathogens, and antibiotic-resistance genes*. In *Current Developments in Biotechnology and Bioengineering*, 79-102.
- ZURBRUGG, C., GFRERER, M., ASHADI, H., BRENNER, W., KUPER, D., 2012. *Determinants of sustainability in solid waste manag. The Gianyar Waste Recovery Project in Indonesia*. *Waste management*, 32, 11, 2126-2133.